Effects of Earth's Rotation on GW Signal Parameter Estimation

Samyak Tiwari

May 9, 2025

Abstract

Michelson interferometry is a laboratory technique that is used for several experiments - forming interference patterns to determine the wavelength of light, studying wind and temperature patterns in the upper atmosphere, and detecting gravitational waves with LIGO. This report explores the latter application, including a first-order approximation of the effect of Earth's rotation on the gravitational wave signals received by LIGO. This approximation is of pressing significance to next-generation detectors, whose longer readable signal lengths require account of the Earth's rotation for proper parameter estimation.

Table of Contents

1 Introduction

When Albert Michelson invented the interferometer in 1881, he hadn't imagined the scale at which it would be used. Designed initially to probe the wave-like nature of light, his invention laid the groundwork for some of the most precise measurement tools in physics. Over time, the interferometer evolved from a tabletop apparatus to a kilometer-scale scientific instrument. Its journey mirrors the trajectory of modern physics itself, from classical mechanics to the frontier of general relativity.

1.1 The Gravitational Wave (GW)

Gravitational waves are spacetime ripples produced by accelerating masses, with compact binary mergers—black holes or neutron stars—among the only sources powerful enough to be detected by LIGO. When two such masses orbit each other, they lose energy to gravitational radiation, and their orbits shrink while their inspiral frequency rises. This makes the gravitational wave signal "chirp" as its frequency and amplitude rise leading to the point of merger, manifesting as perturbations in spacetime.

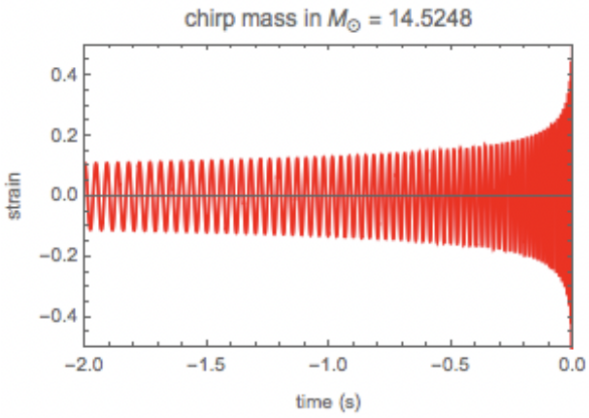

Figure 1: GW Signal Example.[4]

In the linearized theory of general relativity, the spacetime metric $g_{\mu\nu}$ represents the perturbed Minkowski metric $\eta_{\mu\nu}$. That is,

$$g_{\mu\nu} = \eta_{\mu\nu} + h_{\mu\nu}, \quad |h_{\mu\nu}| \ll 1 \tag{1}$$

The perturbation $h_{\mu\nu}$ takes a particularly convenient form for a wave propagating in the z-direction:

$$h_{\mu\nu} = \begin{pmatrix} 0 & 0 & 0 & 0 \\ 0 & h_+ & h_\times & 0 \\ 0 & h_\times & -h_+ & 0 \\ 0 & 0 & 0 & 0 \end{pmatrix}$$

This form reveals two independent polarization modes of the gravitational wave (see Figure 1):

- h_+: the *plus* polarization, which stretches and compresses spacetime along the x- and y-axes.
- $h_\times$: the *cross* polarization, oriented at 45 degrees to the plus mode.

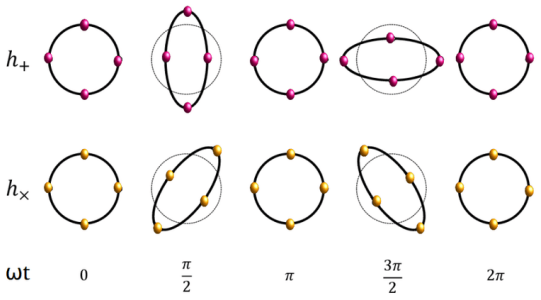

Figure 2: Illustration of gravitational wave polarizations along transverse plane: h_+ and $h_\times$.[1]

Both modes are transverse to the direction of wave propagation (along the z-axis). This is characteristic of gravitational radiation in vacuum.

2 Current GW Signal Model

2.1 What is an interferometer?

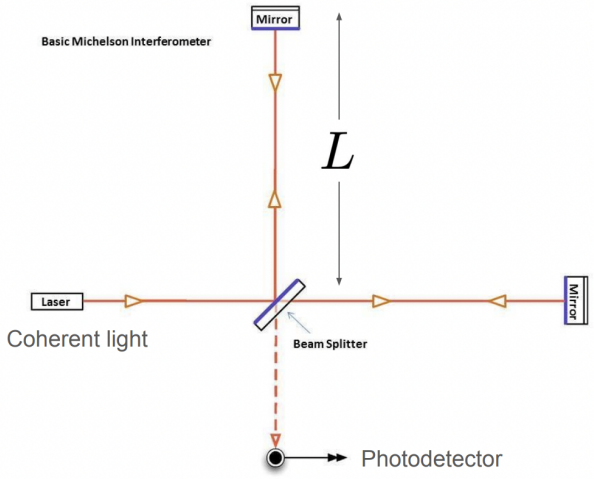

Figure 3: Standard Michelson Interferometer. [3]

An interferometer is a scientific instrument that uses the principle of interference to make precise measurements of displacement. In the case of a Michelson Interferometer, such as those used in LIGO, laser light is split into two beams that travel along perpendicular arms. These beams are reflected back by mirrors and recombined at the photodetector. The resulting interference pattern depends on the difference in the path lengths traveled by the two beams.

The path length difference ΔL between the arms is related to the measured phase difference $\Delta\phi$ by:

$$\Delta L = \frac{\lambda\,\Delta\phi}{2\pi} \tag{2}$$

At its most sensitive state, LIGO is able to detect a change in distance between its mirrors 1/10,000th the width of a proton (10^{-19} m) across its 4km arms [3]! Streams of

strain data $h = \Delta L/L$ are noise-reduced (primarily via high-pass filtering) and masked with a collection of various simulated and real GW signals to detect merger events.

2.2 How are multiple interferometers used?

LIGO-Livingston (the reference detector), LIGO-Hanford, and Virgo are necessarily used together. Each detector's axis orientation determines its sensitivity to the "+" (plus) and "×" (cross) polarization modes of the wave, which are described by the detector-specific response functions F_+ and $F_\times$, respectively. F_+ and $F_\times$ depend on ϕ, the sky angle δ, and the polarization angle ψ.

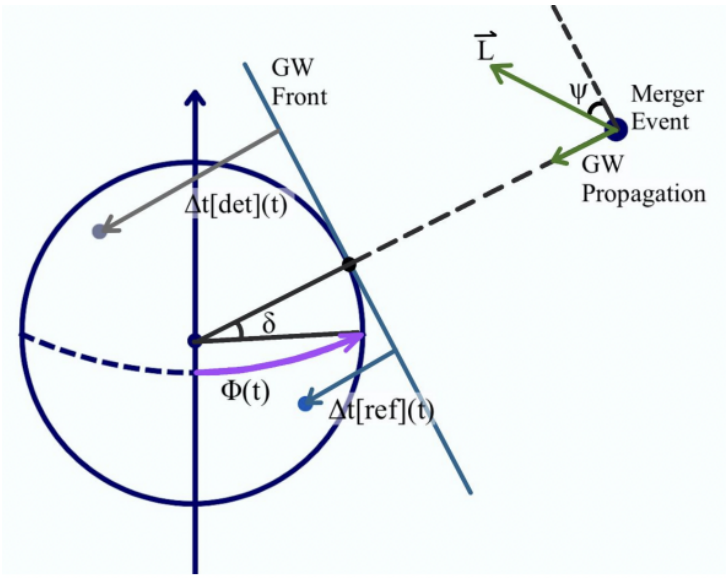

Figure 4: Visual representation of how GW signals are received at Earth. $\phi(t)$ and δ are sky-location angles, while ψ is related to the merger's angular momentum.

In a network of detectors, the arrival time of the GW signal at each site varies due to differences in geographic location. These arrival time differences, denoted Δt, are critical for localizing the GW source on the sky.

The angle $\phi(t)$, representing Earth's rotation, evolves over time as:

$$\phi(t) = \phi_0 + \Omega t \tag{3}$$

where Ω is Earth's rotational rate. In a simplified non-rotating Earth model, $\Omega = 0$, so $\phi(t) = \phi_0$.

In a rotating Earth model (such as the one in Section 3 of this report), all variables dependent on $\phi(t)$ inherit time dependence: $F_+(t)$, $F_\times(t)$, $\Delta t(t)$.

2.3 Zeroth Order (in Ω) GW signal model

The strain $h(t)$ measured by a single detector is a linear combination of the two GW polarization components $h_+(t)$ and $h_\times(t)$, scaled by the detector's response:

$$h(t) = F_+[det] \cdot h_+(t - \Delta t[det]) + F_\times[det] \cdot h_\times(t - \Delta t[det]) \tag{4}$$

Notably, h_+ and $h_\times$ are determined by some set of compact binary merger parameters, θ (further discussed in Section 4).

F_+ and $F_\times$ are given by:

$$F_+ = \vec{X}^T D\vec{X} - \vec{Y}^T D\vec{Y}, \quad F_\times = \vec{X}^T D\vec{Y} + \vec{Y}^T D\vec{X},$$

where D is a 3×3 symmetric, constant matrix describing the detector's orientation and location:

$$D \equiv \begin{pmatrix} D_{11} & D_{12} & D_{13} \\ D_{12} & D_{22} & D_{23} \\ D_{13} & D_{23} & D_{33} \end{pmatrix}.$$

The vectors $\vec{X}$ and $\vec{Y}$ are on the transverse plane of a GW:

$$\vec{X} = \begin{pmatrix} \sin\varphi\cos\psi - \sin\psi\cos\varphi\cos\left(\frac{\pi}{2} - \delta\right), \\ -\cos\varphi\cos\psi - \sin\psi\sin\varphi\cos\left(\frac{\pi}{2} - \delta\right), \\ \sin\psi\sin\left(\frac{\pi}{2} - \delta\right) \end{pmatrix},$$

$$\vec{Y} = \begin{pmatrix} -\sin\varphi\sin\psi - \cos\varphi\cos\psi\cos\left(\frac{\pi}{2} - \delta\right), \\ \cos\varphi\sin\psi - \sin\varphi\cos\psi\cos\left(\frac{\pi}{2} - \delta\right), \\ \cos\psi\sin\left(\frac{\pi}{2} - \delta\right) \end{pmatrix}.$$

The time delay Δt of a given detector (from its reference) is given by:

$$\Delta t[det] = \frac{1}{c}(\vec{r}[det] - \vec{r}[ref]) \cdot e\vec{sr}c, \tag{5}$$

where:

- $\vec{r} = (r_1, r_2, r_3)$ is the location of a detector relative to the center of the Earth
- $e\vec{sr}c$ is the unit propagation vector of the GW, expressed as:

$$e\vec{sr}c = \begin{bmatrix} \cos\left(\frac{\pi}{2} - \delta\right)\cos\lambda \\ \cos\left(\frac{\pi}{2} - \delta\right)\sin\lambda \\ \sin\left(\frac{\pi}{2} - \delta\right) \end{bmatrix}$$

- c is the speed of light

To estimate waveforms, Gaussianity in frequency is assumed of the GW signal (see Section 4). Thus, the GW signal model written in the frequency domain (by taking a Fourier Transform) is relevant:

$$\tilde{h}(f) = \left[F_+[det]\tilde{h}_+(f) + F_\times[det]\tilde{h}_\times(f)\right] e^{-2\pi i f \Delta t[det]} \tag{6}$$

2.4 Why Account for Earth's Rotation?

For current detectors (LIGOs/Virgo), signals typically last $\mathcal{O}(10)$ seconds. During these timescales, Earth's rotation causes only minor variations in detector orientation (F_+, $F_\times$ coefficients) and time delays (Δt between detectors).

However, next-generation detectors will fundamentally change this picture. The GW frequency evolution follows:

$$2\dot{f}_{\rm GW} = \frac{96}{5}\pi^{8/3}\left(\frac{GM}{c^3}\right)^{5/3}(2f_{\rm GW})^{11/3} \tag{7}$$

with M being the chirp mass of a binary merger.

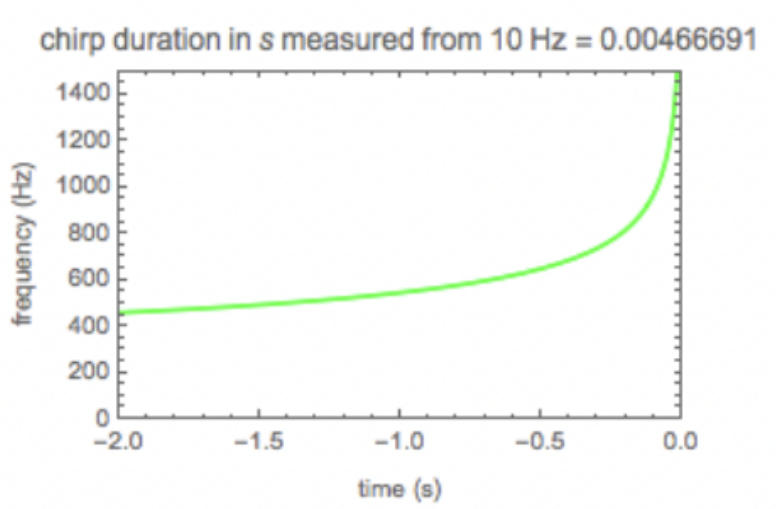

Figure 5: Frequency evolution showing characteristic "chirp" (greater-than-exponential growth) in final moments before merger. Effectively, a plot of Equation (7). [4]

As a result, a seemingly small decrease in the cutoff frequency of a detector (that is, the GW signal can be recovered at lower frequencies) will result in a greater than exponential increase in the detectable signal duration!

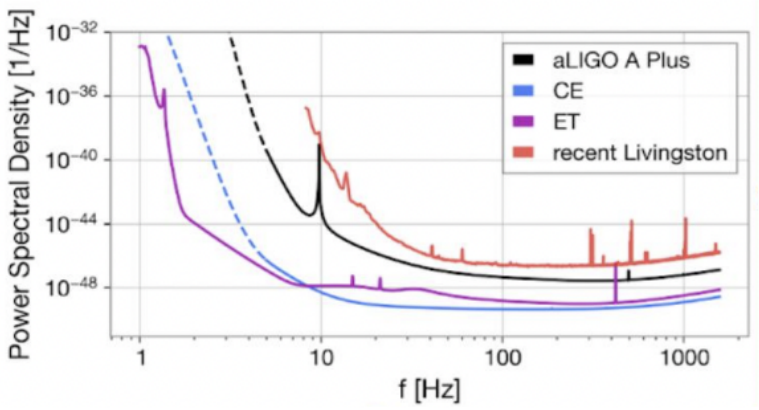

Figure 6: Noise spectra showing improved low-frequency sensitivity [2].

Key differences emerge when comparing detectors:

Parameter	Current	Next-gen
Cutoff frequency	8 Hz	3 Hz
Observable duration	Seconds	Hours

Table 1: Detector capabilities comparison

Thus, with next-gen detectors allowing signal observations on the timescale of hours, Earth's rotation becomes significant.

3 First-Order Perturbative Expansion

3.1 Time Domain Representation

The rotating Earth model introduces time-dependence into all key quantities, including Δt, F_+, and $F_\times$, as:

$$h_{\text{rot}}(t) = F_+[\text{det}](t) \cdot h_+(t - \Delta t[\text{det}](t)) + F_\times[\text{det}](t) \cdot h_\times(t - \Delta t[\text{det}](t)) \tag{8}$$

To account for Earth's rotation, we expand each time-dependent term to first order in Ω, the Earth's rotational rate. This yields linear perturbations around the non-rotating Earth model ($\Omega = 0$):

$$\begin{aligned} F_+(t) &= F_+(t_0) + \Omega \cdot (t - t_0) \cdot \gamma_+, \\ F_\times(t) &= F_\times(t_0) + \Omega \cdot (t - t_0) \cdot \gamma_\times, \\ \Delta t(t) &= \Delta t(t_0) + \Omega \cdot (t - t_0) \cdot \eta, \end{aligned}$$

where γ_+, $\gamma_\times$, and η are constants derived from the detector geometry and source location. Higher-order terms in Ω are neglected in this approximation.

Substituting these expansions into Equation (8) and retaining only first-order terms in Ω, we obtain the first order strain signal perturbation:

$$\begin{aligned} h_{\text{rot}}(t) - h(t) = \Omega \cdot (t - t_0) \cdot \big[& \gamma_+ \cdot h_+(t - \Delta t(t_0)) \\ & - F_+(t_0) \cdot \eta \cdot h'_+(t - \Delta t(t_0)) \big] \\ & + (\text{cross-polarization terms}). \end{aligned} \tag{9}$$

Here, $h(t)$ represents the strain in the non-rotating model, and the additional terms capture the first-order rotational effects. The derivatives h'_+ and $h'_\times$ can be computed numerically via finite-differencing.

3.2 Frequency Domain Representation

To facilitate analysis, we transform the perturbed strain into the frequency domain using key Fourier identities:

$$\begin{aligned} t \cdot x(t) &\xrightarrow{\mathcal{F}} \frac{i}{2\pi} \frac{\partial}{\partial f} \tilde{x}(f), \\ x'(t) &\xrightarrow{\mathcal{F}} 2\pi i f \cdot \tilde{x}(f), \\ x(t - \tau) &\xrightarrow{\mathcal{F}} \tilde{x}(f) \cdot e^{-2\pi i f \tau}. \end{aligned}$$

By defining the following constants to simplify notation:

$$\begin{aligned} \alpha_0 &= e^{-2\pi i f \cdot \Delta t(t_0)}, \\ \alpha_1^+ &= \alpha_0 \cdot \big\{ \eta \cdot \Omega \cdot F_+(t_0) \cdot \big[1 - 2\pi i f \cdot (\Delta t(t_0) - t_0) \big] \\ &\quad + F_+(t_0) + \gamma_+ \cdot \Omega \cdot \big[\Delta t(t_0) - t_0 \big] \big\}, \\ \alpha_2^+ &= \alpha_0 \cdot \Omega \cdot \left\{ \gamma_+ \cdot \frac{i}{2\pi} + \eta \cdot F_+(t_0) \cdot f \right\}. \end{aligned}$$

we arrive at the compact frequency-domain representation of the perturbed strain:

$$\tilde{h}_{\text{rot}}(f) = \alpha_1^+ \cdot \tilde{h}_+(f) + \alpha_2^+ \cdot \tilde{h}'_+(f) + \alpha_1^\times \cdot \tilde{h}_\times(f) + \alpha_2^\times \cdot \tilde{h}'_\times(f). \tag{10}$$

Here, $\alpha_1^\times$ and $\alpha_2^\times$ are analogous to their plus-polarization counterparts, with F_+ and γ_+ replaced by $F_\times$ and $\gamma_\times$, respectively.

4 Conclusion

With readable signal durations on the order of hours, next-generation detectors will require more than a first-order approximation in Ω to obtain closed-form GW signal estimates. That said, the first order approximation, Equation (10), could at least be used to determine the point at which the initial model collapses (that is, when its parameter estimations significantly diverge from the ground truth) — whether as a consequence of a lowered detector frequency cutoff or a reduced binary merger chirp mass (see Equation (7)).

In any case, there remains one thing to (briefly) explore: how is a gravitational wave model used to conduct parameter estimation?

4.1 Parameter estimation

We are given observation $d(f) = h(f) + n(f)$, where $h(f)$ is our GW model and $n(f) \sim N(0, \frac{T}{4} S_n(f))$ under the assumption that noise in our data is Gaussian in the frequency domain. $S_n(f)$ represents the spectral noise density (see Figure 6). We use the following Bayesian parameter estimation framework:

$$P(\theta|d) \propto P(d|\theta) \cdot P(\theta) = L \cdot \text{Prior}$$

where:

- θ represents the merger parameters (chirp mass, spins, location, orientation, tidal deformability for neutron star mergers)
- $P(\theta)$ is the prior probability distribution
- $L \equiv P(d|\theta)$ is the likelihood of observing data d given parameters θ

For GW analysis, we typically work with the log likelihood, which for Gaussian noise in the frequency domain is given by:

$$\log L = \langle d(f)|h(f)\rangle - \frac{1}{2}\langle h(f)|h(f)\rangle \tag{11}$$

where the inner product is defined as:

$$\langle a|b\rangle = \text{Re}\left\{\sum_f \frac{a^*(f)b(f)}{\frac{T}{2} \cdot S_n(f)}\right\}$$

where T is the observation duration.

The posterior distribution $P(\theta|d)$ is typically explored computationally via Markov Chain Monte Carlo (MCMC) methods.

This Bayesian approach allows us to quantify both the most probable parameter values and their uncertainties.

References

[1] Imène Belahcene. *Searching for gravitational waves produced by cosmic strings in LIGO-Virgo data*. PhD thesis, 10 2019.

[2] M. Lazarow, N. Leslie, and L. Dai. A gravitational waveform model for detecting accelerating inspiraling binaries. *arXiv*, 2024. arXiv:2401.04175.

[3] LIGO Laboratory. Ligo's interferometers. https://www.ligo.caltech.edu/page/ligos-ifo, n.d. Accessed: 2025-05-08.

[4] Satya Mohapatra. Newtonian gravitational wave chirp signal from merger of a compact binary. https://demonstrations.wolfram.com/NewtonianGravitationalWaveChirpSignalFromMergerOfACompactBin/, 2011. Wolfram Demonstrations Project.